7-2014

Expression of *Chlorovirus* MT325 aquaglyceroporin (*aqpv1*) in tobacco and its role in mitigating drought stress

Saadia Bihmidine
University of Nebraska-Lincoln

Mingxia Cao
University of Nebraska-Lincoln

Ming Kang
University of Nebraska-Lincoln

Tala Awada
University of Nebraska - Lincoln, tawada2@unl.edu

James L. Van Etten
University of Nebraska - Lincoln, jvanetten1@unl.edu

See next page for additional authors

Authors

Saadia Bihmidine, Mingxia Cao, Ming Kang, Tala Awada, James L. Van Etten, David Dunigan, and Thomas E. Clemente

Expression of *Chlorovirus* MT325 aquaglyceroporin (*aqpv*1) in tobacco and its role in mitigating drought stress

Saadia Bihmidine,
School of Natural Resources, University of Nebraska-Lincoln, Lincoln, NE 68583-0968, USA

Mingxia Cao,
Department of A gronomy and Horticulture, Center for Plant Science Innovation, University of Nebraska-Lincoln, Lincoln, NE 68588-0660, USA

Ming Kang,
Department of Plant Pathology, Nebraska Center for Virology, University of Nebraska-Lincoln, Lincoln, NE 68583-0900, USA

Tala Awada,
School of Natural Resources, University of Nebraska-Lincoln, Lincoln, NE 68583-0968, USA

James L. Van Etten,
Department of Plant Pathology, Nebraska Center for Virology, University of Nebraska-Lincoln, Lincoln, NE 68583-0900, USA

David D. Dunigan, and
Department of Plant Pathology, Nebraska Center for Virology, University of Nebraska-Lincoln, Lincoln, NE 68583-0900, USA

Tom E. Clemente
Department of A gronomy and Horticulture, Center for Plant Science Innovation, University of Nebraska-Lincoln, Lincoln, NE 68588-0660, USA, tclemente1@unl.edu

Abstract

Main conclusions A Chlorovirus aquaglyceroporin expressed in tobacco is localized to the plastid and plasma membranes. Transgenic events display improved response to water deficit. Necrosis in adult stage plants is observed.

Aquaglyceroporins are a subclass of the water channel aquaporin proteins (AQPs) that transport glycerol along with other small molecules transcellular in addition to water. In the studies communicated herein, we analyzed the expression of the aquaglyceroporin gene designated, *aqpv1*, from *Chlorovirus* MT325, in tobacco (*Nicotiana tabacum*), along with phenotypic changes induced by *aqpv1* expression *in planta*. Interestingly, *aqpv1* expression under control of either a constitutive or a root-preferred promoter, triggered local lesion formation in older leaves, which

progressed significantly after induction of flowering. Fusion of a*qpv1* with GFP suggests that the protein localized to the plasmalemma, and potentially with plastid and endoplasmic reticulum membranes. Physiological characterizations of transgenic plants during juvenile stage growth were monitored for potential mitigation to water dry-down (i.e., drought) and recovery. Phenotypic analyses on drought mimic/recovery of juvenile transgenic plants that expressed a functional *aqpv1* transgene had higher photosynthetic rates, stomatal conductance, and water use efficiency, along with maximum carboxylation and electron transport rates when compared to control plants. These physiological attributes permitted the juvenile *aqpv1* transgenic plants to perform better under drought-mimicked conditions and hastened recovery following re-watering. This drought mitigation effect is linked to the ability of the transgenic plants to maintain cell turgor.

Keywords

Aquaporins; Aquaglyceroporins; Water use efficiency; *Agrobacterium*; Local lesions; Chlorovirus MT325

Introduction

Components of plant water relations include soil water availability, uptake and transport through the root system to the aerial part of the plant. Water conductance *in planta*, uses three primary routes, (1) apoplastic movement wherein water translocates intercellular without crossing membranes, (2) symplastic movement whereby cell-to-cell transport of water molecules occurs via plasmodesmata and (3) a transcellular route in which water molecules move through water-specific channel proteins (Chrispeels and Maurel 1994; Maurel and Chrispeels 2001; Maurel et al. 2008; Steudle and Peterson 1998). Water channel proteins are members of the major intrinsic proteins (MIPs) family, that collectively are referred to as aquaporins (AQPs) when they are exclusively water channels or as aquaglyceroporins when transported molecules also include glycerol and other small molecules (Eckert et al. 1999; Maurel and Chrispeels 2001; Maurel et al. 2008; Schaffner 1998; Tyerman et al. 2002). Plant AQPs are further subdivided into four subgroups classified by subcellular localization, plasmalemma intrinsic proteins, tonoplast intrinsic proteins, nodulin-26-like intrinsic membrane proteins and small basic proteins (Alexandersson et al. 2005; Maurel et al. 2008; Peng et al. 2007).

Some dsDNA viruses that infect algae (family *Phycodnaviridae*) have genomes of up to 560 kb and contain as many as 600 protein-encoding genes including ion channels and ion transporters (Van Etten and Dunigan 2012). An example is the *Chlorovirus* MT325 that infects *Micractinium conductrix* (former name *Chlorella* Pbi). The MT325 open reading frame (ORF) M30R encodes an aquaglyceroporin protein (AQPV1) that has MIP like features and the capacity to transport both water and glycerol (Gazzarrini et al. 2006). *Xenopus* oocytes injected with AQPV1 transcripts displayed significantly higher water permeability than corresponding control oocytes in a hypotonic swelling assay. Moreover, a single point mutation in AQPV1 abolished the activity of the protein channel with respect to water permeability, which demonstrated that a functional pore was required for water transport (Gazzarrini et al. 2006). The AQPV1 gene call was through in silico analyses of

the MT325 sequence. However, information on the expression or subcellular localization of aqpv1 protein in virus-infected *Chlorella* has not been ascertained.

This report describes the expression of *aqpv1* in tobacco and subsequent phenotypic characterizations under water limiting conditions. While transgenic approaches to elucidate the role of AQPs in plant water relations have been reported (Lian et al. 2004; Peng et al. 2007; Sade et al. 2010; Wang et al. 2011), this is the first report describing *in planta* heterologous expression of a viral aquaglyceroporin channel.

Materials and methods

Vector constructions

The coding sequence of *aqpv1* from *Chlorovirus* MT325 (genbank acc no. DQ195162) was amplified via PCR from virus DNA. The PCR reaction incorporated an *Nco*I and *Xba*I site at the 5′ and 3′ ends of the ORF, respectively. The primer set used was aqua5: 5′-TTCATGGCCACTTA CACCTCCTCCAGATT -3′ and aqua3: 5′-TTCTA GATTAAATCGCAAAGGAAGTGATC -3′. The PCR reaction incorporated an Ala residue at the N-terminus between the Met and Thr residues. The PCR product was subsequently cloned into TOPO 2.1 cloning vector (TOPO TA cloning kit® Invitrogen Cat No. K4510) and sequenced to verify authenticity of the PCR product. The *Nco*I/*Xba*I element containing the *aqpv1* ORF was subcloned into pRTL 2 (Carrington and Freed 1990), which fuses the ORF to the tobacco etch virus translational enhancer element (TEV), and places expression of the transgene TEV fusion under control of the 35S CaMV promoter. The resultant plasmid is referred to as pPTN798 (not shown). The 35S CaMV *aqpv1* expression cassette was subcloned from pPTN798 as a *Pst*I element into the base binary vector pPZP211 (Hajdukiewicz et al. 1994) with the final binary plasmid designated pPTN803 (Fig. 1). The TEV-*aqpv1* element was also placed under control of the *Arabidopsis* root-preferred promoter Pyk10 (Nitz et al. 2001), by swapping the 35S CaMV promoter out from pPTN798 as a *Hin*dIII/*Xho*I and replacing it with the Pyk10 promoter delineated by *Hin*dIII/*Xho*I sites. The final binary plasmid carrying this second TEV-*aqvp1* expression cassette under control of the Pyk10 promoter is referred to as pPTN817 (Fig. 1).

Two additional control vectors were assembled. The first binary control vector, designated pPTN814 (Fig. 1) had a GUSPlus™ cassette derived from pCambia 1304 in which the GUSPlus gene, fused to the TEV leader, is under control of the *Arabidopsis* pyk10 promoter. This plasmid was used to monitor pyk10 promoter activity in tobacco. The second control plasmid had a N214A mutation in the AQPV1 peptide, which abolishes both water and glycerol transport (Gazzarrini et al. 2006). The mutation was generated using a QuickChange® site-directed mutagenesis kit (Stratagene Cat No. 200518) following the protocol outlined by the manufacturer. The primer set aqF: 5′-GACTTCAATTGC TGCGCGCACGTGATTTCTC -3′ and aqR: 5′-GAGAAATCACGTGCGGGGGCGGCAGCAATTGAA GTC-3′ was used in the reaction with plasmid pPTN798 serving as the template. The plasmid carrying the mutated *aqpv1* gene cassette is designated pPTN839 (not shown). The fidelity of the targeted change was confirmed by sequencing. The mutated expression cassette in pPTN839 was subsequently subcloned into pPZP211 and the final binary vector referred to as pPTN841 (Fig. 1).

To visualize subcellular localization of AQPV1 in tobacco, a GFP fusion protein was generated, in which the C-terminal end of the full-length AQPV1 peptide was linked to the visual marker. To this end primer sets, aqua- BspHI: 5′-TCATGACTTACAACCTCCTCCAGATTT -3′, aqua-RV: 5′-GATATCAATCGCAAAGGAAGTGATCTC GG-3′, GFP-RV: 5′-GATATCATGTCCAAGGGCGAACT CTC-3′ and GFP-Xba: 5′-TCTAGACTACTTGTAGAGCT CGTCATGCCGTG -3′ were used to amplify the *aqpv1* ORF and a synthetic GFP ORF, using the aqua and GFPlabeled primer sets, respectively. The *aqpv1*-GFP fusion N-terminus does not have an Ala residue between the Met and Thr, and the linker region of the peptide is Phe-Ala-Asp-Ile-Met. Hence, the AQPV1 C-terminus of the fusion is replaced with Asp-Ile, rather than Tyr-Leu in the native peptide. The *aqvp1*-GFP fusion was cloned into pRTL 2 as described above, as a *Bsp*HI/*Xba*I element, and the resultant plasmid, designated pPTN834 (not shown) was confirmed by sequencing. The 35S CaMV-TEV-aqvp1-GFP cassette was subsequently cloned into pPZP211 and the final binary vector referred to as pPTN836 (Fig. 1).

Tobacco transformations

Tobacco transformations (*Nicotiana tabacum* cv. Xanthi) were conducted using a modification of the protocol described by Horsch et al. (1985). A detailed procedure of the tobacco transformation protocol usedin this study was previously communicated (Clemente 2006).

Molecular characterizations of transgenic tobacco events

A subset of the pPTN803 transgenic events was characterized at the molecular level to monitor both integration patterns and transcript accumulation of the *aqpv1* transgene. The former was determined via Southern blot analysis on selected progeny of transgenic plants. Total genomic DNA was extracted from young leaves during vegetative growth using a modification of the protocol described by Dellaporta et al. (1983). 10 μg of genomic DNA was digested with *Kpn*I, which contains one recognition site in the T-DNA. The digested DNA s were subsequently separated on a 0.8 % agarose gel. The gels were blotted to a nylon membrane (Bio-Rad, Hercules, CA) following a series of deamination and denaturation steps, the DNA s were crosslinked to the membrane with a UV-crosslinker. Hybridizations were carried out with ^{32}P-labeled dCTP using the *aqpv1* ORF in the random prime synthesis reaction following the manufacturer's protocol (Prime-It II, Stratagene, La Jolla, CA). Membrane pre-hybridizations and hybridization conditions were carried out as previously described (Eckert et al. 2006).

Transcript accumulation was monitored via northern blot analysis. Total RNA s were isolated from young leaves during vegetative growth using TRIzol® reagent (Life Technologies, Grand Island, NY, USA), and subsequently purified using RNeasy columns (Qiagen, German Town, MD, USA). Approximately 15 μg of RNA s were separated on a 1 % formaldehyde agarose gel. The gel was subsequently blotted to a nylon membrane and pre-hybridization and hybridization conditions followed as above, using the *aqpv1* ORF as a probe.

Confocal imaging

Subcellular localization of AQPV1 was visualized in transgenic tobacco plants harboring the T-DNA of pPTN836. Images were captured with an Olympus FV500 laser scanning confocal microscope. Imaging analysis was conducted at the University of Nebraska's Morrison Microscopy Core Research Facility. Images were acquired with a 60× objective. Two channel, simultaneous images of GFP and plastid autofluorescence images were captured with 488 and 633 nm laser excitation and 505–524 nm and 660 nm long pass emission filters, respectively.

Water stress experimental design

Water stress studies were carried out using two independent pPTN803-derived transformants designated aqua3-1 and aqua4-12, along with three controls, wild-type (WT) Xanthii, a vector control transgenic event, harboring T-DNA of the base binary plasmid pPZP211 (Hajdukiewicz et al. 1994) and a transgenic event derived from pPTN841, referred to as aqua841-2. All studies were carried out using T_2 or T_3 populations of the various transgenic plants. Two treatments were created, "well-watered" and "dry-down" (drought mimic). In the former, plants were watered to soil saturation throughout the study period, while in the latter water was withheld until photosynthesis and stomatal conductance values approached zero before plants were re-watered and allowed to recover. Plant physiological and growth measurements were monitored at 2- or 3-day intervals prior to the initiation of the dry-down treatment (day 0), and during dry-down/recovery times.

Due to the destructive nature in monitoring growth and development, a split-plot in time experimental design was followed. Three subsets of plants were sampled at three time periods during each experiment: prior to initiation of dry-down, the last day of dry-down, and after recovery. A second set of plants was used only for leaf water status measurements. These measurements are considered semidestructive due to leaf sampling that triggers changes in water balance, and wounding stress. To avoid potential confounding data due to leaf detachment, pots were arranged as a split-plot design in time with repeated measurements within a period on different set of plants throughout each experiment. Leaves were sampled prior to initiation and during the first half of the dry-down period, a second sampling of leaves was carried out during the second half of the dry-down period, and a third sampling of leaves occurred during the recovery phase. As measurements of leaf gas exchange are non-destructive, plants in this part of the experiments were arranged in a randomized factorial design with repeated measurements over time. Hence for each experiment, three sets of plants were set up in the greenhouse; two sets were arranged in a split-plot design, while the third was placed as a randomized factorial.

Measured parameters

Gas exchange measurements were conducted using a portable infrared gas analyzer system mounted with a fluorescence chamber (LI-6400, Li-Cor Inc. Lincoln, NE, USA). Maximum net photosynthesis (A_{net}, μmol m^{-2} s^{-1}), stomatal conductance (g_s, mol m^{-2} s^{-1}), transpiration rates (E, mmol m^{-2} s^{-1}), and instantaneous water use efficiency (iWUE = A_{net}/E, μmol mol^{-1}) were followed at light saturation (photosynthetic active radiation, PAR 1,250 μmol m^{-2} s^{-1}) determined from running initial photosynthetic light response curves.

The rates of maximum electron transport (J_{max}, µmol m^{-2} s^{-1}) and maximum carboxylation efficiency (V_{cmax}, µmol m^{-2} s^{-1}) were derived from A_{net}/C_i curves. These curves were created following the protocol previously described (Long and Bernacchi 2003), using leaf chamber CO_2 concentrations (C_a) of 2,500, 2,000, 1,500, 1,000, 800, 600, 400, 300, 100 and 50 µmol mol^{-1}. Net photosynthesis (A_{net}) was first measured at ambient greenhouse CO_2 concentration (C_a 400 µmol mol^{-1}), after which the concentrations were lowered stepwise to 300, 200, 100, and 50 µmol mol^{-1}, with A_{net} recorded at each level. Following the 50 µmol mol^{-1} reading, C_a was returned to 400 µmol mol^{-1}, and A_{net} ascertained for validation before stepwise monitoring to 2,500 µmol mol^{-1} (Bihmidine et al. 2010; Long and Bernacchi 2003; Xu and Baldocchi 2003). Both V_{cmax} and J_{max} were then determined from each A_{net}/C_i curve by non-linear regression using the A_{net}/C_i curve fitting utility (Sharkey et al. 2007). The maximum photochemical efficiency of photosystem II (Fv/Fm) was determined on dark-adapted leaves using a leaf fluorometer attached to the LI-6400 infrared gas analyzer. Minimal or dark-adapted chlorophyll fluorescence (F_o) occurs when all PSII reaction centers are open, and maximal fluorescence (F_m) occurs when all reaction centers are closed. The variable fluorescence (F_v) was tabulated by the difference between F_o and F_m. When measured in the dark, F_v/F_m is proportional to the maximum potential quantum yield of photosynthesis (Bihmidine et al. 2010). Chlorophyll fluorescence was measured on older leaves, adapted to dark for at least 30 min using dark-adapting clips (Li-Cor Inc. Lincoln, NE, USA).

Water status determination

Midday leaf water potential (Ψ_w, MPa) was determined using a PMS 1000 pressure chamber (PMS Instrument Co., Albany OR, USA). Osmotic potential was calculated from the Van't Hoff equation $\Psi_\Pi = -RTc$, where R (J mol^{-1} K^{-1}) is the universal gas constant, T (K) is the temperature, and c (mol m^{-3}) is the molar concentration of the solutes obtained using a vapor pressure osmometer (Vapro 5520, Wescor, Logan UT, USA, Nobel 2009).

Growth parameters

Growth-related parameters including total number of leaves (NL), total leaf dry weight (DW$_{TL, g}$), above-ground dry weight (DW$_{AG, g}$), total leaf area (LA$_t$, cm^2), and specific leaf area (SLA, cm^2 g^{-1}) were determined. The LI-3100C leaf area meter (Li-Cor Inc. Lincoln, NE, USA) was used to measure total LA$_t$ of the plants and SLA was ascertained by the ratio of LA$_t$ to DW$_{TL}$.

Statistical analysis

The statistical analysis package R v. 2.14 (R Development Core team, 2012) was used to fit generalized linear models with gamma distributions and log link functions (Crowley 2005; Faraway 2006) to data for the continuous response variables. The model consisted of additive and interacting parameters for plant, line, and day either since initiation of drought exposure or during continued watering for control plants. The contrast package v0.17 for R v. 2.14 (R Development Core Team, 2012) was used to conduct pairwise comparisons with one-degree-of-freedom Wald tests (Kuhn et al. 2011). The variable "day" was converted

from numeric to a categorical variable to allow for pairwise comparisons (p 0.05) of plants on a day-specific means within treatments (watered versus exposed to dry-down).

Results

Genotyping and phenotyping evaluation of transgenic pPTN803 tobacco events were carried out on lineages from selected independent transgenic events. Southern analysis on 14 such lineages is shown in Fig. 2a. Given that a single *Kpn*I recognition site resides within T-DNA of pPTN803, each hybridization signal corresponds to a genetic locus, which may have one to many copies. Integration patterns reveal that between one and five *aqpv1* transgenic loci are present in the plants. One of the plants, designated Aqua4-6, was positive for the selectable marker *nptII* (data not shown) but the *aqpv1* transgenic allele was not detected.

Transcript accumulation in vegetative tissue is shown in Fig. 2b for the two pPTN803 events Aqua3-1and Aqua4-12. The northern blot analysis revealed a strong hybridizing signal in the transgenic plants and absence of a corresponding signal in the non-transgenic control (WT). The transgenic plants, grown to maturity under greenhouse conditions, were phenotypically indistinguishable from control, non-transgenic Xanthii during vegetative growth. However, at the onset of flowering, necrotic lesions formed in older leaves, starting at the base of the plant and progressively moved toward the apex (Fig. 3). The severity of this necrosis phenotype varied among the transgenic events; however, all pPTN803 events ultimately developed symptoms. However, we were unable to correlate transcript profiling with lesion severity given the northern analysis was more qualitative rather than quantitative and the transgenic events in which northern analysis was conducted were relatively strong in expression.

We rationalized that organ-specific expression of *aqpv1* might be responsible for the onset of necrosis during the juvenile to adult stage transition in the aerial portion of the plants. To explore this possibility we selected the root/ seedling preferred promoter that regulates expression of an *Arabidopsis* myrosinase gene, designated *Pyk10* (Nitz et al. 2001), to control *aqpv1* transgene expression. The *Pyk10 aqpv1* expression cassette resides in the binary vector designated pPTN817 (Fig. 1). Twelve to 15 independent tobacco transgenic plants were produced. Genotyping of all derived plants from transformations with pPTN817 was not conducted; hence, we are assuming some genetic clones were established in the greenhouse. However, like the constitutive 35S CaMV AQPV1 cassette (pPTN803), necrotic lesions appeared at the onset of flowering, with a deeper penetrance at the base of the plant (compare Fig. 4a to b). Moreover, the root systems of these plants were severely reduced in robustness, and darkened in color (Fig. 4c) as compared to controls (Fig. 4d).

To monitor the Pyk10 promoter activity directly in tobacco we constructed a GUSPlus™ expression cassette (pPTN814, Fig. 1). Histochemical staining for GUS (Jefferson 1987) revealed that the Pyk10 regulatory element is essentially constitutive in tobacco, with intense GUS staining observed in roots, leaves and flowers of the transgenic tobacco plants (Fig. 4e, f). This finding probably explains the similarity of the progressive necrotic lesion phenotype during the induction of flowering in the transgenic Pyk10-*aqpv1* plants (pPTN814) with plants containing the constitutive *aqpv1* cassette (pPTN803).

To determine if a functional aquaglyceroporin is required to induce formation of the necrotic lesions during the transition from juvenile to adult stage in tobacco, we constructed a single point mutation at AQPV1 codon 214 that changed the asparagine residue to an alanine (N214A). This N214A mutation was previously shown to make AQPV1 non-functional as a water transport channel (Gazzarrini et al. 2006). The N214A *aqvp1* transgene was assembled into an expression cassette and subsequently subcloned into a binary vector designated pPTN841 to resemble the constitutive cassette harbored in pPTN803 (Fig. 1). Transgenic tobacco plants carrying the N214A *aqvp1* constitutive transgene cassette accumulated transcripts as monitored by northern blots at levels equal to the transgenic events expressing the native *aqpv1* gene (data not shown) and plant development proceeded normally without forming necrotic lesions. Hence, the logical explanation for these results is that a biologically active AQPV1 is required for lesion formation in adult plants.

To investigate the subcellular localization of AQPVI *in planta* a GFP fusion cassette was assembled and the final binary vector was designated pPTN836 (Fig. 1). GFP expression was monitored via confocal microscopy in a subset of the transgenic events. The images suggest that AQPV1 is located in the plasmalemma, with possible association with plastids and endoplasmic reticulum (Fig. 5). However, a plastid transit peptide was not detected in the N-terminal region of the AQPV1 protein. The elucidation of the actual subcellular location of the channel was hindered due to the relative weak GFP expression in the transgenic events carrying the AQPV1 fusion. The transgenic tobacco plants carrying this fusion, albeit low expressing based on GFP imaging, like the non-fusion AQPV1 plants, formed necrotic lesions in older leaves of adult plants (data not shown).

Given the appearance of necrotic lesions in older leaves during the juvenile to adult stage transition in transgenic plants expressing AQPV1, we restricted our investigations on mitigation of mimicked drought stress to juvenile stage plants. Plants used in the study included two independent events derived from pPTN803 (AQPV1), one event from pPTN841 (*aqpv1* N214A), a transgenic control group designated 744d-6 which harbors a T-DNA carrying two unrelated transgenic cassettes, along with WT non-transgenic plants. Therefore, a total of five tobacco lines were used; two test transgenic events, two control transgenic events, and one wild-type non-transgenic line.

The effect of *aqpv1* expression on leaf gas exchange was monitored by measuring A_{net}, g_s and E in the transgenic events. Under well-watered conditions A_{net}, g_s and E did not differ significantly (p 0.05) between plants expressing *aqpv1* and control plants throughout the study period (Fig. S1). The rates of A_{net}, g_s and E varied between 14.3 and 17.9 μmol m^{-2} s^{-1}, 0.083 and 0.135 mol m^{-2} s^{-1} and 3.8 and 7.9 mmol m^{-2} s^{-1}, respectively.

A_{net}, g_s, and E at light saturation declined in response to soil dry-down (drought mimic) as expected, reaching minimal values on day 4 for E, and day 9 for A_{net} and g_s, of water deprivation, before they commenced the recovery process after re-watering on day 10 (Fig. 6). Photosynthesis in the pPTN803 transgenic events did not differ from controls after 2 days of dry-down. However, by day 4 the transgenic *aqpv1* events maintained significantly higher A_{net} (p 0.05) than controls. This observation of maintained A_{net} rates under water deprivation was observed through day 9, which translated into enhanced photosynthetic

performance during the dry-down and faster recovery from stress after re-watering in the transgenic *aqpv1* plants as compared to controls (Fig. 6). Stomatal conductance followed a similar trend to A_{net}. However, significant differences between the transgenic pPTN803 events and controls did not appear until day 7 of water deprivation (Fig. 6). With respect to E rates, no significant differences were observed among the plants tested, until day 9 of water deprivation, contributing to higher water use efficiency (iWUE = A_{net}/E) in the two *aqpv1* plants (Table S1).

Leaf water and osmotic potentials

Variations in both leaf water (Ψ_w) and osmotic (Ψ_Π) potentials were minimal in plants under well-watered conditions and only few differences were observed (data not shown). For example, plant Aqua3-1 had a significantly lower Ψ_Π as compared to WT and control plant 744d-6 at day 2, while control plant Aqua841-2 had reduced Ψ_Π at the initiation of the study, day 0, compared to the rest of the lines (data not shown).

Soil water dry-down resulted in a significant (p 0.05) decline in both Ψ_w and Ψ_Π (Fig. 7) across all plants. Significant declines were observed on day 4 for Ψ_Π in all plants, and on day 7 for Ψ_w in controls. Significant declines in Ψ_w were not observed till day 9 for *aqpv1* plants (Fig. 7). Importantly, significantly higher Ψ_w rates were maintained 7 and 9 days after the initiation of the dry-down treatment and throughout the recovery period (Fig. 7a). Overall the *aqpv1* events Aqua3-1 and Aqua4-12 displayed enhanced Ψ_Π compared to the controls throughout the study (Fig. 7b), suggesting that *aqpv1* improved water status of the plant during the stress period by maintaining better leaf turgor than control plants. This improvement is further supported by regressing A_{net} as a function of Ψ_w (Fig. S2), which revealed that Ψ_w in the *aqpv1* events did not fall below −1 MPa throughout the dry-down period, and maintained higher rates of A_{net} at lower Ψ_w values compared to the respective controls.

Rates of J_{max} and V_{cmax}

To investigate the impact of *aqpv1* expression *in planta* on maximum rates of electron transport (J_{max}) and rubisco carboxylation (V_{cmax}), A_{net}/C_i curves were created. Due to the time limitation required for a single curve, and the challenge to obtain reliable curves under increasing water stress, replication became an issue in developing the curves. To address the replication issue, and thus allow for proper statistical analyses, an assumption was made that under well-watered conditions V_{cmax} and J_{max} rates did not differ significantly and therefore data were complied across the study time frame for each line (Tables S1, S2). In addition, for the dry-down treatment, there were many cases in which only one reliable curve was obtained (i.e., one data point) per date assayed within each event/control, hence, no statistical analysis was carried out in these cases (Tables S1, S2; Fig. S3). Nonetheless, the results obtained from the data indicate that the estimated maximum rates of J_{max} and V_{cmax} were higher in the *aqpv1* events as compared to the controls, with a higher positive trajectory after 8 days of water deprivation through the recovery phase of the study (Tables S1, S2; Fig. S3). For example, at day 8 of water deprivation, V_{cmax} was estimated at 15.87 and 16.09 μmol m^{-2} s^{-1}, with J_{max} values of 42.42 and 30.3 μmol^{-2} s^{-1} for Aqua3-1 and Aqua4-12 plants, respectively. The control event 744d-6 had a V_{cmax} of 6.52 μmol m^{-2} s^{-1},

and a $J_{\max}$ of 21.25 μmol m^{-2} s^{-1}; reliable A_{net}/C_i curves were not obtained with the other controls, WT and the Aqua841-2 event, hence the absence of data points (Tables S1, S2; Fig. S3). Nonetheless, even considering the missing data points for two of the controls, taken together these results with the other datasets, suggest that leaves of the *aqpv1* plants maintained enhanced turgor, rubisco carboxylation, and electron transport, which translates to improved tolerance to water stress relative to the controls.

Plant biomass, growth and development

During this study various biomass-related parameters were also monitored, including total number of leaves (NL), leaf dry weight (DW$_{\mathrm{TL}}$), above-ground dry weight (DW$_{\mathrm{AG}}$), total leaf area (LA$_t$), and specific leaf area (SLA). The data are tabulated in Tables S1 and S2. No statistical differences were observed when comparing biomass parameters between the *aqpv1* plants and the controls under well-watered conditions (Table S2). As expected various parameters were impacted by the dry-down treatment (Table S1). Following 9 days of water deprivation, the *aqpv1* events displayed higher DW$_{\mathrm{TL}}$ and DW$_{\mathrm{AG}}$, and lower SLA compared to the controls. Hence, the observed enhancement of various physiological parameters did translate moderately into biomass.

Although only modest enhancement occurred in some of the biomass parameters, which is likely related to the brief exposure to stress imposed during the study, the *aqpv1* events had a significant delay in wilting relative to the controls (Fig. S4). The delay in wilting phenotype was most pronounced at the 9 day dry-down time (Fig. S4).

Discussion

The various components of plants water relations, from soil absorption through *in planta* translocation, are highly regulated throughout development. The maintenance of water homeostasis at both the intracellular and the whole plant levels is a challenge when individuals are exposed to environmental conditions that limit water availability. The water status of plants associated with movement across biological membranes is regulated by AQPs, hence, under water stress conditions coordination of AQPs *in planta* is paramount for plant survival (Maurel et al. 2008; Quigley et al. 2001). Elucidation of the mechanism(s) coordinating the network of AQPs' governing water relations of plants under water sufficient and depleted environments has great potential for developing genetic approaches to enhance water use efficiency and mitigating the impact of drought stress on agronomic performance of crop plants.

The underlying biology governing the influence of AQPs on plant water relations is complicated by the dual regulation of AQPs at both transcriptional and post-translational levels. Previous investigations monitoring transcript accumulation of AQPs under water stress, summarized in the review by Tyerman et al. (2002), reveal both up- and downexpression patterns in various tissues for both tonoplastic and plasmalemma localized AQPs. The functional modulation of properly subcellular localized AQPs is mediated by phosphorylation (Törnroth-Horsefield et al. 2006). This dual regulation at transcriptional and post-translational levels, coupled with, in some cases, tissue-type coordinated

localization (Prado et al. 2013) is the apparent underlying process that plays a significant role in a plant's water status.

The ability to modulate gene expression by plant transformation is a powerful approach for gaining insight into gene function and coordination of biological processes such as water relations. To this end, previous studies have used transgenic approaches to understand water status and various abiotic stresses of plants by specifically overexpressing or down-regulating targeted AQPs. Examples include: (1) heterologous expression of a barley plasmalemma AQP, *Hv*PIP2;1 in rice led to reduction in salt tolerance in transgenic plants with modest phenotypic changes under control conditions (Katsuhara et al. 2003). (2) Heterologous expression of a ginseng tonoplast localized AQP, *Pg*TIP1, resulted in improved salt tolerance and changes in root lengths, which translated into alterations in drought responses in transgenic *Arabidopsis* plants (Peng et al. 2007). (3) Ectopic expression of the tonoplastic localized *At*Tip5;1 resulted in boron tolerance in *Arabidopsis* plants (Pang et al. 2010). (4) Transgenic tobacco plants expressing the *Arabidopsis* AQP PIP1b exhibited positive phenotypic changes under well-watered conditions with respect to physiological parameters including transpiration rates and photosynthetic capacity; these physiological changes translated into enhanced biomass, but these positive phenotypes were not displayed under water- or salt-stress conditions (Aharon et al. 2003).

One unexpected observation from this study was the induction of lesion formation in transgenic tobacco plants expressing an active form of *aqpv1*. A cursory mineral analysis was conducted on leaf tissue harvested from selected plants at both juvenile and adult stages, with the latter displaying lesion formation. While some variation in leaf accumulation of various minerals was observed, for example Ca levels were reduced in juvenile leaves of *aqpv1* events and Mn accumulation was, in general, reduced in transgenic *aqpv1* plants, as compared to control tissues (Table S3), the subtle changes in mineral accumulation were not likely the underlying cause that led to cell death.

In addition to the mineral analysis we monitored both glycerol content (BioVision free glycerol kit Cat # K630-100) and fatty acid profiles in vegetative tissues of juvenile stage plants from representative transgenic plants Aqua3-1, Aqua4-12, 841-2 (N214A mutant) along with a WT control in an attempt to gain insight into the underlying cause that triggered lesion formation. No significant differences were detected (data not shown) among the selected tobacco lines either in glycerol content, fatty acid profile or fatty acids levels. While these data did not reveal the cause of lesion induction, one possible clue might lie in the possible *aqpv1* subcellular association with plastids and other cellular membranes (Fig. 5). Given that aquaglyceroporins can transport a plethora of molecules, including nitrogen compounds, metals, hydrogen peroxide, carbon dioxide and glycerol (Bhattacharjee et al. 2008; Bienert et al. 2007; Luu and Maurel 2013; Uehlein et al. 2008), it is reasonable to suggest that altered intracellular water and/or solute homeostasis via changes in permeability of plastid and/or ER membrane(s) may have either altered cellular retrograde signaling from plastids (Mullineaux 2009) and/or triggered an endoplasmic reticulum stress response (Howell 2013), which in turn triggered the cell death cascade. However, this is merely conjecture without confirmatory studies to resolve the subcellular location(s) of *aqpv1 in planta*.

We measured leaf chlorophyll fluorescence by monitoring rates of maximum efficiency of photosystem II (Fv/Fm) in older leaves located at the base of adult stage transgenic plants in which lesion formation was induced. The relationship between Fv/Fm and Ψ_w revealed that the *aqpv1* transgenic plants displayed lower rates of Fv/Fm and have a more negative Ψ_w than corresponding controls (Fig. S5). These data reflect the impaired function of the photosynthetic apparatus in the leaves with lesions.

The potential of *aqpv1* to mitigate drought stress was investigated in juvenile stage tobacco plants. Under wellwatered conditions no significant differences were found for the parameters measured. However, under droughtmimicked conditions, *aqpv1* mitigated some of the expected water stress impacts through maintenance of higher Ψ_w and Ψ_Π along with A_{net}, g_s and iWUE, essentially leading to improved turgor in the transgenic events as compared to the corresponding controls which in turn facilitated maintenance of physiological processes in the plant. In addition, under the dry-down treatment, the *aqpv1* plants displayed higher DW_{TL} and DW_{AG}, and reduced SLA along with a delay in wilting as compared to the respective controls. SLA (leaf area/dry weight) is known to decrease in response to drought, due to water stress impacts on leaf expansion, cell size and cell division, this is especially noticeable in expanding leaves, such as our case (Liu and Stutzel 2003). The higher DW_{TL} and DW_{AG} and lower SLA observed in the *aqpv1* plants relative to controls, probably contributed to improved turgor, which led to moderate biomass accumulation relative to leaf area, resulting in decline in the overall SLA.

In summary, the viral aquaglyceroporin AQPV1 localizes to both plasmalemma and plastid membranes in tobacco plants. Incorporation of this channel in the respective membranes clearly impacts the physiology of the plant that results in a measurable mitigation of drought stress response in young plants, but with an unexpected induction of cell death as the plant transitions to the adult stage. These results reflect the importance of maintaining proper water/solute relations *in planta* and the need for a deeper understanding of the coordinated functional of AQPs before a rational genetic design to combat stress responses can be implemented successfully in a breeding program.

Supplementary Material

Refer to Web version on PubMed Central for supplementary material.

Acknowledgments

References

Aharon R, Shahak Y, Wininger S, Bendov R, Kapulnik Y, Galili G. Overexpression of a plasma membrane aquaporin in transgenic tobacco improves plant vigor under favorable growth conditions but not under drought or salt stress. Plant Cell. 2003; 15:439–447. [PubMed: 12566583]

Alexandersson E, Fraysse L, Sjovall-Larsen S, Gustavsson S, Fellert M, Karlsson M, Johanson U, Kjellbom P. Whole gene family expression and drought stress regulation of aquaporins. Plant Mol Biol. 2005; 59:469–484. [PubMed: 16235111]

Bhattacharjee H, Mukhopadhyay R, Thiyagarajan S, Rosen BP. Aquaglyceroporins: ancient channels for metalloids. J Biol. 2008; 7:33. [PubMed: 19014407]

Bienert GP, Møller ALB, Kristiansen KA, Schulz A, Møller IM, Schjoerring JK, Jahn TP. Specific aquaporins facilitate the diffusion of hydrogen peroxide across membranes. J Biol Chem. 2007; 282:1183–1192. [PubMed: 17105724]

Bihmidine S, Bryan NM, Payne KR, Parde KR, Okalebe JA, Cooperstein SE, Awada T. Photosynthetic performance of invasive *Pinus ponderosa* and *Juniperus virginiana* seedlings under gradual soil water depletion. Plant Biol. 2010; 12:668–675. [PubMed: 20636910]

Carrington JC, Freed DD. Cap-independent enhancement of translation by a plant potyvirus 5′ nontranslated region. J Virol. 1990; 64:1590–1597. [PubMed: 2319646]

Chrispeels MJ, Maurel C. Aquaporins: the molecular basis of facilitated water movement through living plant cells? Plant Physiol. 1994; 105:9–13. [PubMed: 7518091]

Clemente T. Nicotiana (*Nicotiana tobaccum*, *Nicotiana benthamiana*). Methods Mol Biol. 2006; 343:143–154. [PubMed: 16988341]

Crowley, MJ. Statistics: an introduction using R. Wiley; England: 2005. p. 155-185.

Dellaporta SL, Wood J, Hicks JB. A plant DNA minipreparation: version II. Plant Mol Biol Report. 1983; 1:19–21.

Eckert M, Biela A, Siefritz F, Kaldenhoff R. New aspects of plant aquaporin regulation and specificity. J Exp Bot. 1999; 50:1541–1545.

Eckert H, LaVallee B, Schweiger BJ, Kinney AJ, Cahoon EB, Clemente T. Co-expression of the borage ^{6} desaturase and the Arabidopsis ^{15} desaturase results in high accumulation of stearidonic acid in the seeds of transgenic soybean. Planta. 2006; 224:1050–1057. [PubMed: 16718484]

Faraway, JJ. Extending the linear model with R: generalized linear, mixed effects and nonparametric regression models. Chapman & Hall/CRC; USA: 2006.

Gazzarrini S, Kang M, Epimashko S, Van Etten JL, Dainty J, Thiel G, Moroni A. Chlorella virus MT325 encodes water and potassium channels that interact synergistically. Proc Natl Acad Sci USA. 2006; 103:5355–5360. [PubMed: 16569697]

Hajdukiewicz P, Svab Z, Maliga P. The small, versatile *pPZP* family of *Agrobacterium* binary vectors for plant transformation. Plant Mol Biol. 1994; 25:989–994. [PubMed: 7919218]

Horsch RB, Fry JE, Hoffmann NL, Eichholtz D, Rogers SG, Fraley RT. A simple and general method for transferring genes into plants. Science. 1985; 227:1229–1231. [PubMed: 17757866]

Howell SH. Endoplasmic reticulum stress responses in plants. Annu Rev Plant Biol. 2013; 64:477–499. [PubMed: 23330794]

Jefferson RA. Assaying chimeric genes in plants: the GUS gene fusion system. Plant Mol Biol Rep. 1987; 5:387–405.

Katsuhara M, Koshio K, Shibasaka M, Hayashi Y, Hayakawa T, Kasamo K. Over-expression of a barley aquaporin increased the shoot/root ratio and raised salt sensitivity in transgenic rice plants. Plant Cell Physiol. 2003; 44:1378–1383. [PubMed: 14701933]

Kuhn, M.; Weston, S.; Wing, J.; Forester, J. [13 April 2012] Contrast: a collection of contrasts methods. R package version 0.17. 2011. http://cran.rproject.org/package=contrast

Lian HL, Yu X, Ye Q, Ding X, Kitagawa Y, Kwak SS, Su WA, Tang ZC. The role of aquaporin RWC3 in drought avoidance in rice. Plant Cell Physiol. 2004; 45:481–489. [PubMed: 15111723]

Liu F, Stutzel H. Biomass partitioning, specific leaf area, and water use efficiency of vegetable amaranth (*Amaranthus* spp.) in response to drought stress. Sci Hortic. 2003; 102:15–27.

Long SP, Bernacchi CJ. Gas exchange measurements, what can they tell us about the underlying limitations to photosynthesis? Procedures and sources of error. J Exp Bot. 2003; 54:2393–2401. [PubMed: 14512377]

Luu D-T, Maurel C. Aquaporin trafficking in plant cells: an emerging membrane-protein model. Traffic. 2013; 14:629–635. [PubMed: 23425337]

Maurel C, Chrispeels MJ. Aquaporins. A molecular entry into plant water relations. Plant Physiol. 2001; 125:135–138. [PubMed: 11154316]

Maurel C, Verdoucq L, Luu DT, Santoni V. Plant aquaporins: membrane channels with multiple integrated functions. Ann Rev Plant Biol. 2008; 59:595–624. [PubMed: 18444909]

Mullineaux, P. ROS in retrograde signalling from chloroplast to the nucleus. In: del Río, LA.; Puppo, A., editors. Reactive oxygen species in plant signaling, signaling and communication in plants. Springer; Berlin Heidelberg: 2009. p. 221-240.

Nitz I, Berkefeld H, Puzio PS, Grundler FMW. Pyk10, a seedling and root specific gene and promoter from *Arabidopsis thaliana*. Plant Sci. 2001; 161:337–346. [PubMed: 11448764]

Nobel, PS. Physiochemical and environmental plant physiology. Academic Press/Elsevier; San Diego: 2009.

Pang Y, Li L, Ren F, Lu P, Wei P, Cai J, Xin L, Zhang J, Chen J, Wang X. Overexpression of the tonoplast aquaporin AtTIP5;1 conferred tolerance to boron toxicity in *Arabidopsis*. J Genet Genomics. 2010; 37:389–397. [PubMed: 20621021]

Peng Y, Lin W, Cai W, Arora R. Overexpression of a *Panax ginseng* tonoplast aquaporin alters salt tolerance, drought tolerance and cold acclimation ability in transgenic *Arabidopsis* plants. Planta. 2007; 226:729–740. [PubMed: 17443343]

Prado K, Boursiac Y, Tournaire-Roux C, Monneuse J-M, Postaire O, Da Ines O, Schäffner AR, Hem S, Santoni V, Maurel C. Regulation of *Arabidopsis* leaf hydraulics involves light-dependent phosphorylation of aquaporins in veins. Plant Cell. 2013; 25:1029–1039. [PubMed: 23532070]

Quigley F, Rosenberg JM, Shahar-Hill Y, Bonhert HJ. From genome to function: the *Arabidopsis* aquaporins. Genome Biol. 2001; 3:1–17.

Sade N, Gebretsadik M, Seligmann R, Schwartz A, Wallach R, Moshelion M. The role of tobacco Aquaporin1 in improving water use efficiency, hydraulic conductivity, and yield production under salt stress. Plant Physiol. 2010; 152:245–254. [PubMed: 19939947]

Schaffner AR. Aquaporin function, structure, and expression: are there more surprises to surface in water relations? Planta. 1998; 204:131–139. [PubMed: 9487723]

Sharkey TD, Bernacchi CJ, Farquhar GD, Singsaas EL. Fitting photosynthetic carbon dioxide response curves for C_3 leaves. Plant Cell Environ. 2007; 30:1035–1040. [PubMed: 17661745]

Steudle E, Peterson CA. How does water get through roots? J Exp Bot. 1998; 49:775–788.

Törnroth-Horsefield S, Wang Y, Hedfalk K, Johanson U, Karlsson M, Tajkhorshid E, Neutze R, Kjellbom P. Structural mechanism of plant aquaporin gating. Nature. 2006; 439:688–694. [PubMed: 16340961]

Tyerman SD, Niemietz CM, Bramley H. Plant aquaporins: multifunctional water and solute channels with expanding roles. Plant Cell Environ. 2002; 25:173–194. [PubMed: 11841662]

Uehlein N, Otto B, Hanson DT, Fischer M, McDowell N, Kaldenhoff R. Function of *Nicotiana tabacum* aquaporins as chloroplast gas pores challenges the concept of membrane CO_2 permeability. Plant Cell. 2008; 20:648–657. [PubMed: 18349152]

Van Etten JL, Dunigan DD. Chloroviruses: not your everyday plant virus. Trends Plant Sci. 2012; 17:1–8. [PubMed: 22100667]

Wang X, Li Y, Ji W, Bai X, Cai H, Zhu D, Sun XL, Chen LJ, Zhu YM. A novel *Glycine soja* tonoplast intrinsic protein gene responds to abiotic stress and depresses salt and dehydration tolerance in transgenic *Arabidopsis thaliana*. J Plant Physiol. 2011; 168:1241–1248. [PubMed: 21397356]

Xu L, Baldocchi DD. Seasonal trends in photosynthetic parameters and stomatal conductance of blue oak (*Quercus douglasii*) under prolonged summer drought and high temperature. Tree Physiol. 2003; 23:865–877. [PubMed: 14532010]

Abbreviations

AQPs	Aquaporins
AQPV1	Aquaglyceroporin protein virus1

MIPs	Major intrinsic proteins
ORF	Open reading frame
A_{net}	Net photosynthesis (μmol m^{-2} s^{-1})
g_s	Stomatal conductance (mol m^{-2} s^{-1})
E	Transpiration (mmol m^{-2} s^{-1})
PAR	Photosynthetic active radiation (μmol m^{-2} s^{-1})
iWUE	Instantaneous water use efficiency (μmol mol^{-1})
J_{max}	Maximum election transport rate (μmol m^{-2} s^{-1})
V_{cmax}	Maximum carboxylation efficiency (μmol m^{-2} s^{-1})
Fv/Fm	Maximum photochemical efficiency of photosystem II
F_o	Minimal or dark-adapted chlorophyll fluorescence
F_m	Maximal fluorescence
F_v	Variable fluorescence
Ψ_{Π}	Osmotic potential (MPa)
Ψ_w	Water potential (MPa)
NL	Total number of leaves
DW_{TL}	Total leaf dry weight (g)
DW_{AG}	Above-ground dry weight (g)
LA_t	Total leaf area (cm^2)
SLA	Specific leaf area (cm^2 g^{-1})
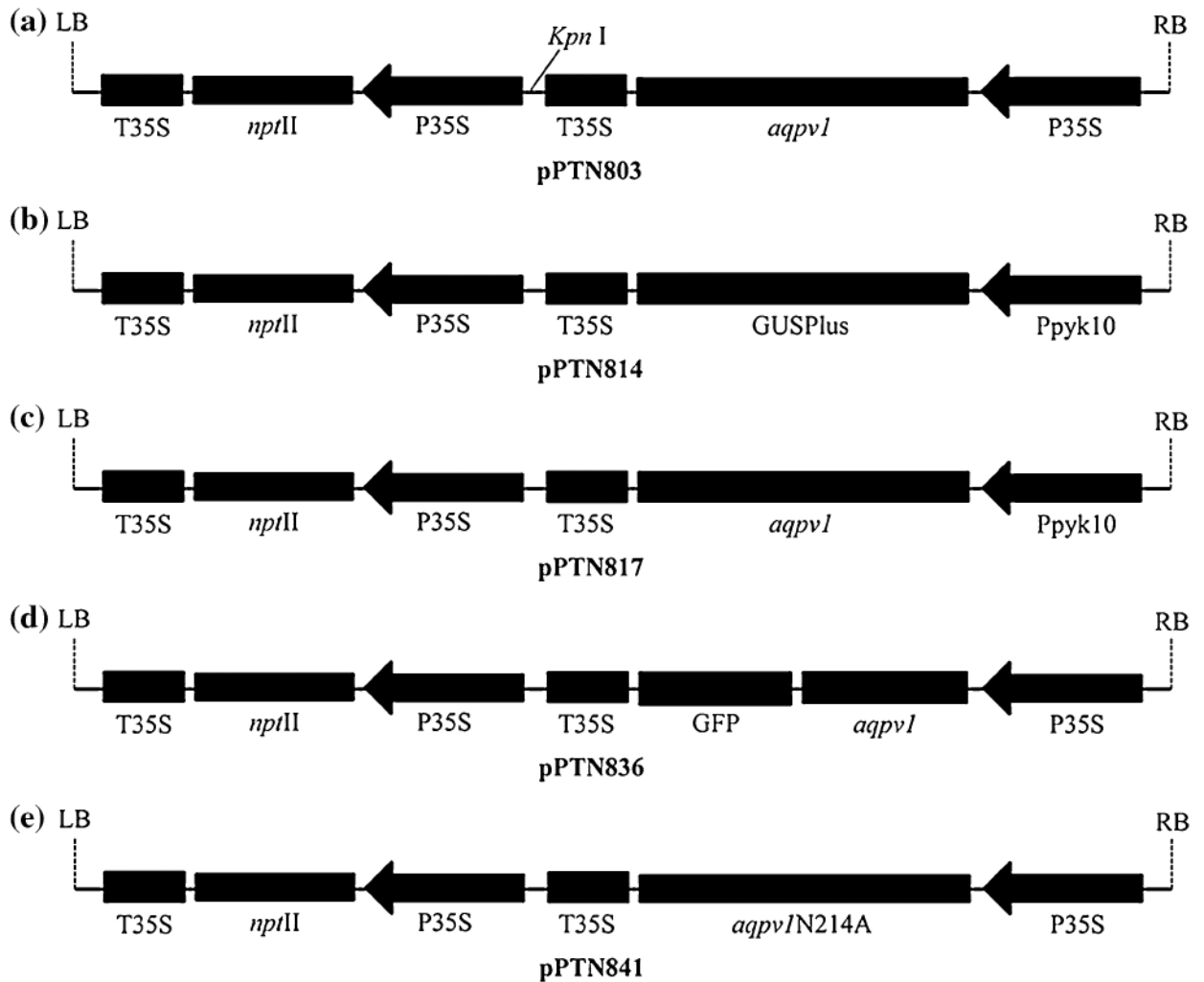
Fig. 1.
Diagrams of T-DNA elements from the binary plasmids used in this study. **a** T-DNA element of pPTN803, **b** T-DNA element of pPTN814, **c** T-DNA element of pPTN817, **d** T-DNA element of pPTN836, and **e** T-DNA element of pPTN841. LB and RB refer to *left* and *right* border elements, respectively. P35S and T35S indicate the positions of the 35S CaMV promoter and terminator sequences, respectively. The marker gene is *nptII* (neomycin phosphotransferase II). **a** highlights a unique KpnI restriction site used during Southern blot analysis of selected plants
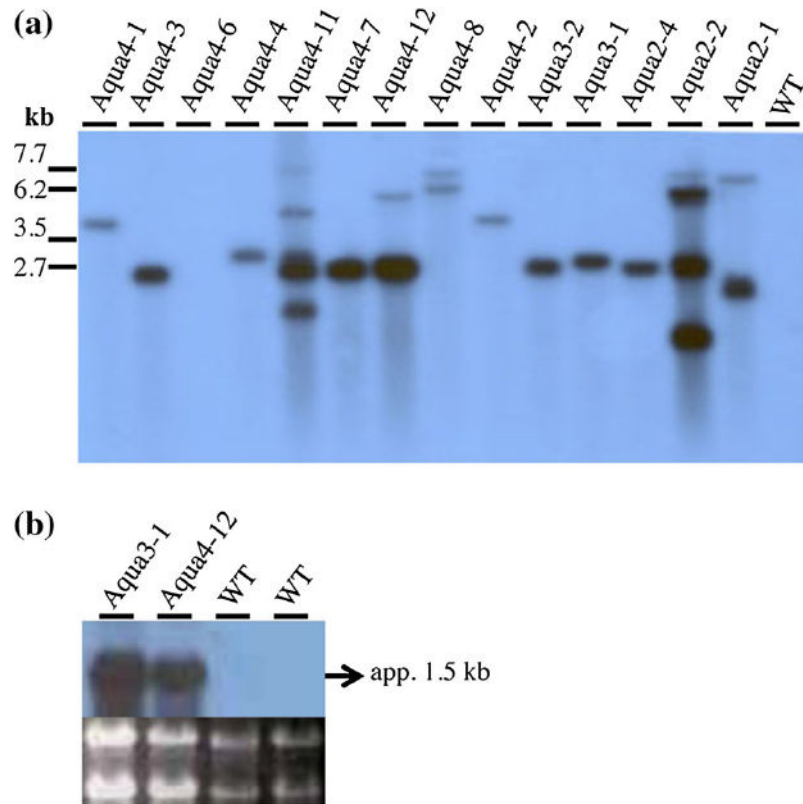
Fig. 2.
Southern blot and northern blot analyses of selected tobacco events. **a** Southern blot analysis on selected plants. Total genomic DNA was cleaved with *KpnI* and DNA s hybridized with *AQPV1* ORF. WT lane refers to control non-transgenic genomic DNA. **b** Northern blot analysis showing *AQPV1* transcript accumulation in events Aqua3-1 and Aqua4-12. *Bottom* panel is the corresponding gel image

Fig. 3.
Tobacco plants Aqua4- 12 and 841-2 at flowering stage. **a** Tobacco plant Aqua4-12 showing necrosis in vegetative tissues at flowering stage of development (*left*) and plant 841-2 harboring the N214A mutation (*right*). Panels **b** and **c** show close-up of a leaf from Aqua4-12 and 841-2, respectively

Fig. 4.
Tobacco plants harboring Pky10 promoter-regulated cassettes. **a** Tobacco plant Aqua15-4
has the Pky10 promoter *aqpv1* cassette in binary vector pPTN817. **b** Control wild-type
tobacco at flowering grown side-by-side under greenhouse conditions with the plant in (**a**).
Panels **c** and **d** show root mass corresponding to plants shown in **a** and **b**, respectively.
Panels **e** and **f** display histochemical GUS staining of various tissues of a transgenic tobacco
plant carrying the Pky10-GusPlus cassette within binary vector pPTN814. **e** Leaf (*left*) and
roots (*right*) **f** from *left* to *right*, roots, leaf, and floral tissues
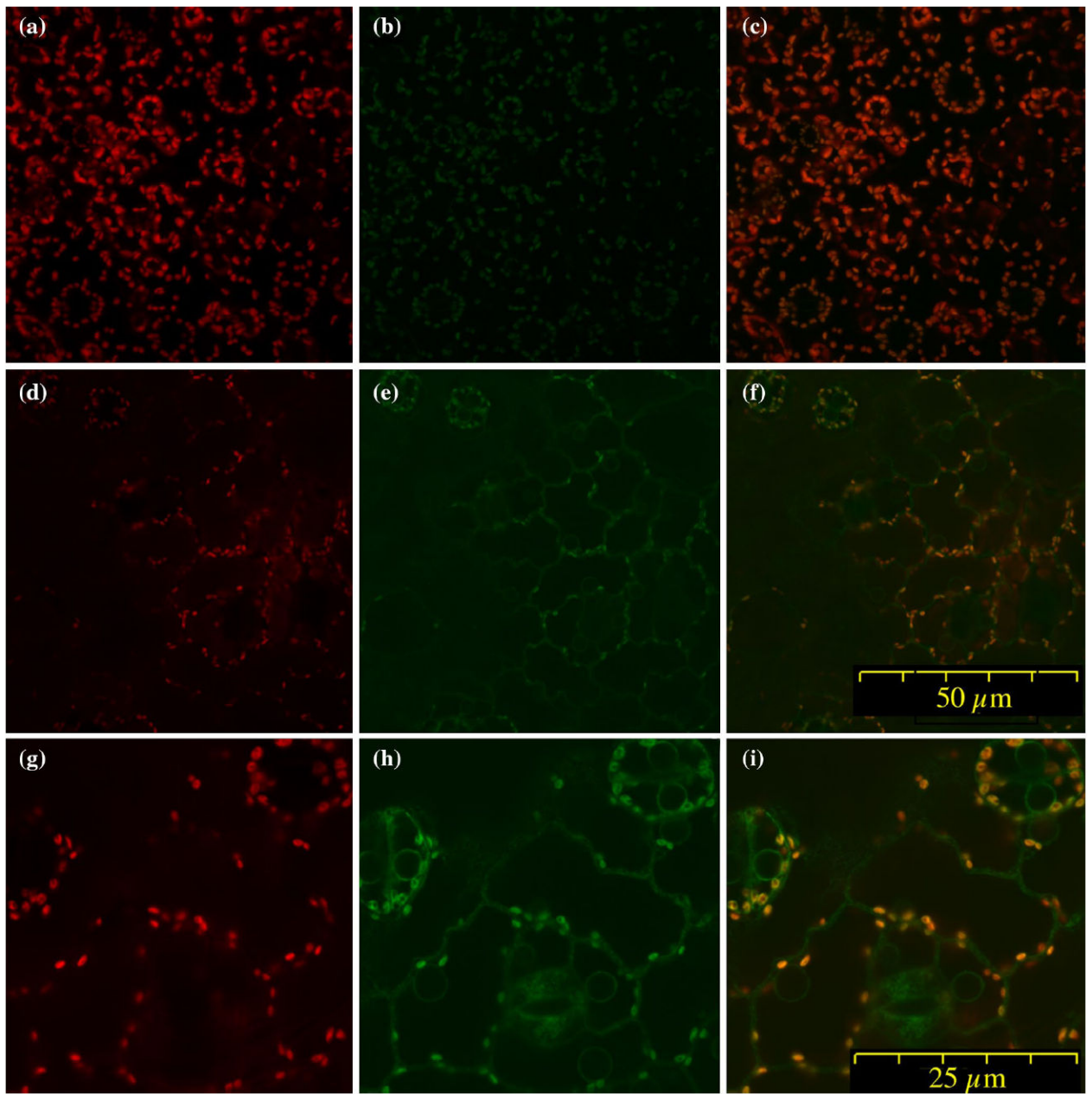
Fig. 5.
Confocal images of a tobacco plant with the *aqvp1*-GFP fusion. Panels **a** through **c** correspond to *red* channel, *green* channel and merged images, respectively, observed in control. wild-type tobacco. Panels **d, e** and **f** correspond to *red* channel, *green* channel and merged images observed in tobacco event 836-11 which is expressing the aqpv1-gfp fusion (pPTN836). Panels **g, i** and **j** are *red* and *green* channels, along with merged images, respectively, of the transgenic pPTN836 event expressing the aqpv1-gfp fusion magnified 2×
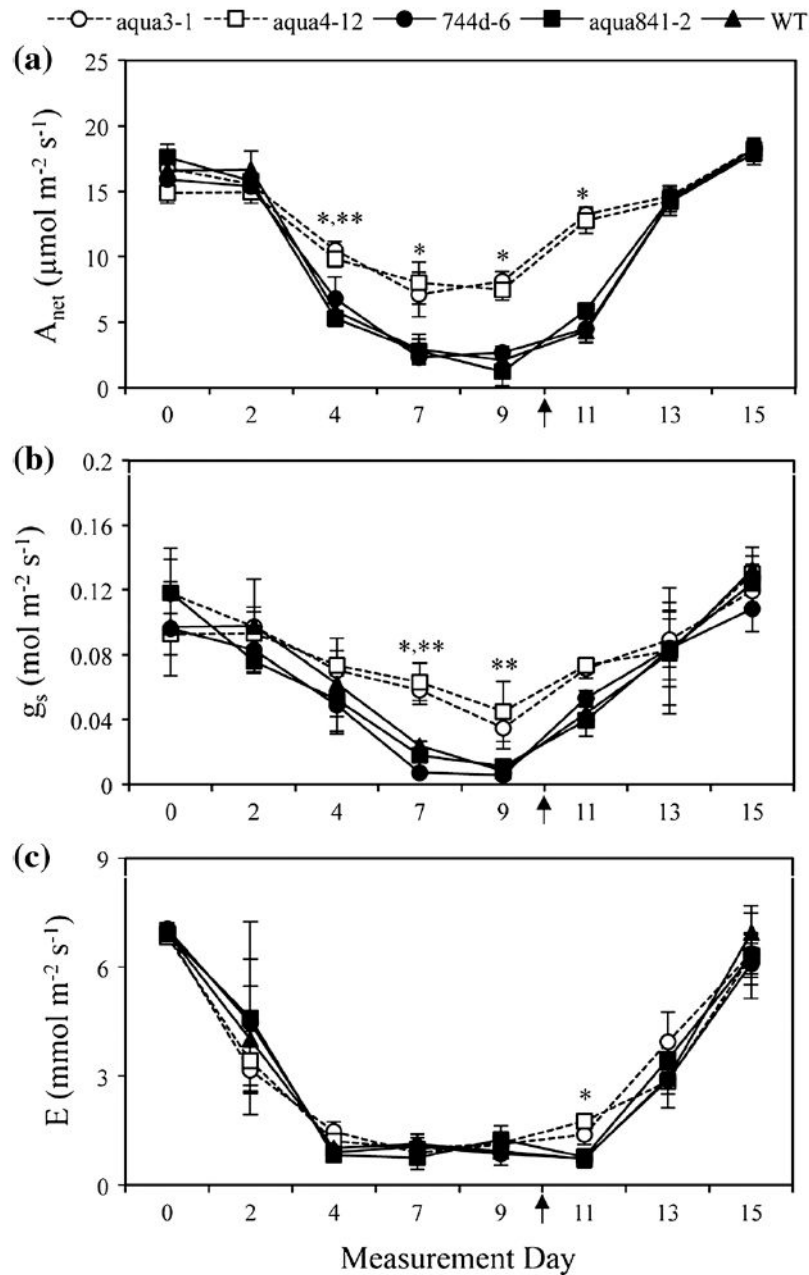
Fig. 6.
Physiological parameters monitored during the dry-down experiment. **a** Net photosynthesis (A_{net}, μmol m^{-2} s^{-1}), **b** stomatal conductance (g_s, mol m^{-2} s^{-1}), and **c** leaf transpiration (E, mol m^{-2} s^{-1}) at light saturation (PAR = 1,250 μmol m^{-2} s^{-1}) of tobacco plants exposed to drought stress followed by a period of recovery. Values are mean ± SE of $n = 3$, and an *asterisk* indicates a significant difference between at least one of the two *aqpv1* and one control line within a given date at *p 0.05 or **p 0.1. Note: plant 744d-6 is a transgenic control carrying the *nptII* marker gene cassette and unrelated gene of interest
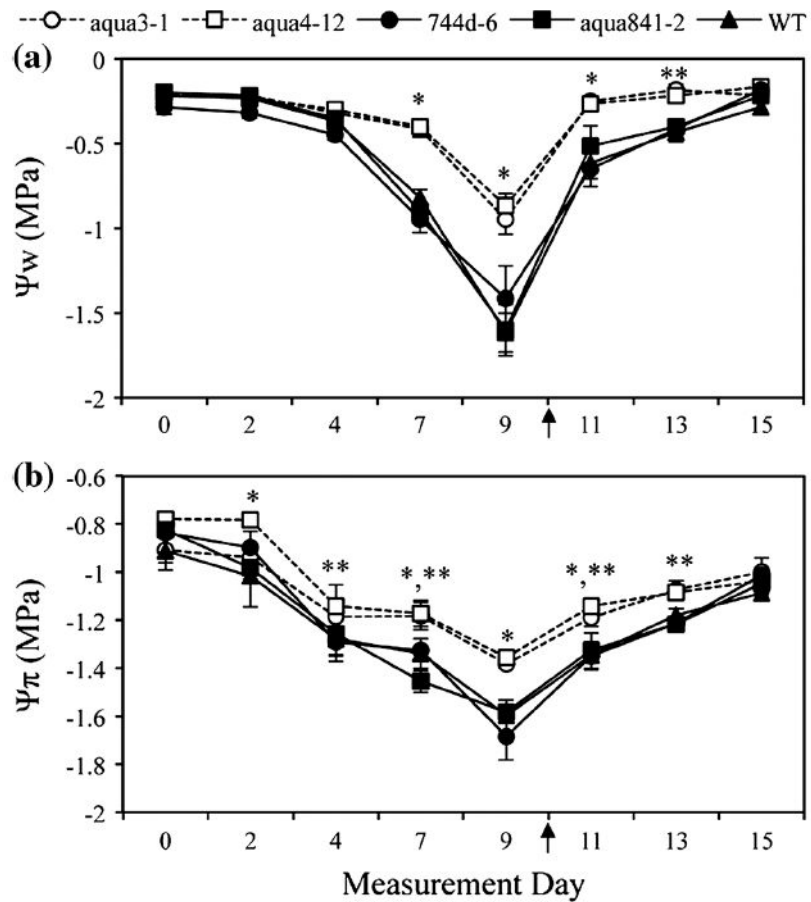
Fig. 7.
Leaf water and osmotic potential monitored during the drydown experiment. **a** Leaf water
(Ψ_w, MPa) and **b** osmotic potential (Ψ_Π, MPa) of tobacco plants during drought followed by
a recovery period. Values are mean ± SE of $n = 3$, and an *asterisk* indicates significant
difference between at least one of the two *aqpv1* plants and one control line within a given
date at *p 0.05 or **p 0.1. Note: plant 744d-6 is a transgenic control carrying the *nptII*
marker gene cassette and an unrelated gene